Electronic Supplementary Information

Controlled Assembly of Organic Whispering-Gallery-Mode Microlasers as Highly Sensitive Chemical Sensors

Miaomiao Gao, ‡[a] Cong Wei, ‡[b] Xianqing Lin,[b] Yuan Liu,[a] Fengqin Hu*[a] and Yong Sheng Zhao*[b]

[a] *Beijing Key Laboratory of Energy Conversion and Storage Materials, College of Chemistry, Beijing Normal University, Beijing 100875, China. E-mail: fqhu@bnu.edu.cn*

[b] *Key Laboratory of Photochemistry, Institute of Chemistry, Chinese Academy of Sciences, Beijing 100190, China, University of Chinese Academy of Sciences, Beijing 100049, China. E-mail: yszhao@iccas.ac.cn*

‡ *M. Gao and C. Wei contributed equally to this work.*

Contents

i. **Experimental section**

ii. **Fig. S1.** Fluorescence quantum yield of F8BT film.

iii. **Fig. S2.** SEM images of the polymer microspheres with different diameters.

iv. **Fig. S3.** Photoluminescence spectra of F8BT microspheres and F8BT thin film.

v. **Fig. S4.** Principle illustration of the chemical vapor sensors based on the organic WGM microlaser.

vi. **Fig. S5.** The luminescence responses of the passive and active microcavities on acetone vapor.

vii. **Fig. S6.** The response of the microsphere sensors to different kinds of organic chemical vapors.

viii. **Fig. S7.** Response detection under different pressures.

ix. **Fig. S8.** Lasing spectra from the microlaser sensor in air and a magnified view of the highest intensity lasing peak.

x. **Fig. S9.** Acetone dose response of the microspheres with different diameters.

xi. **Fig. S10.** Photograph of the F8BT microemulsion.

xii. **Fig. S11.** Schematic demonstration of the experimental setup for the optical sensing measurements.

Experimental section

Preparation: Poly(9,9-dioctylfluorene-alt-benzothiadiazole) (F8BT) and cetyl trimethyl ammonium bromide (CTAB) were purchased from Aldrich Chemical Co., and used without further purification. The microspheres were prepared through a surfactant-assisted microemulsion self-assembly method. In a typical preparation, 200 μL F8BT solution (12.5 mg/mL) in good solvent of chloroform was added into 500 μL CTAB aqueous solution (0.7 mg/mL) to form an oil-in-water emulsion (Fig. S8) under continuous stir at room temperature. After aging for 1 h, the $CHCl_3$ was totally evaporated and F8BT microspheres was obtained and dispersed in the colloid solution. After that, the colloid solution were washed with water to remove the excess CTAB and filtered through a 0.45 micron pore size membrane filter. Finally, the precipitate was redispersed in water and was then used to prepare samples for further characterizations by drop-casting.

Characterization: The morphology of the polymer spheres was examined by scanning electron microscopy (SEM, FEI Nova NanoSEM 450). The absorption and fluorescence spectra were measured on a UV-visible spectrometer (Perkin-Elmer Lambda 35) and a fluorescent spectrometer (Hitachi F-7000), respectively. The spatially resolved spectra were measured with a grating monochrometer (Princeton Instrument Acton SP 2300i; 600 grooves/mm with a corresponding spectral resolution of 0.1 nm) connected with an EMCCD (Princeton Instrument ProEM 1600B). PL microscopy images were taken with an inverted microscope (Nikon, Ti-U).

FDTD simulation: we used a home-made FDTD code for the numerical simulations. The size of the simulation region was 4000×4000 nm^2 with a background refractive index corresponding to that of air, and the refractive index of the disk (D=2000 nm) was set to 1.98, which was adopted to simulate the spatial distribution of mode profile around the equator of the microsphere. Randomly distributed and polarized electric dipoles were adopted to simulate the electromagnetic effects of randomly distributed dye molecules inside the experimental microspheres. In order to phenomenologically describe the surrounding gas's influence on the electric field distribution of the WGM cavity, we assume that the gas molecule disperse homogeneously and isotropically around the outer surface of the microsphere to simplify the computational model. Therefore, a shell layer

(100 nm) with single refractive index of the gas (n=1.36) enwrapping the microsphere was taken to simulate the gas influence on the electric field in FDTD simulation.

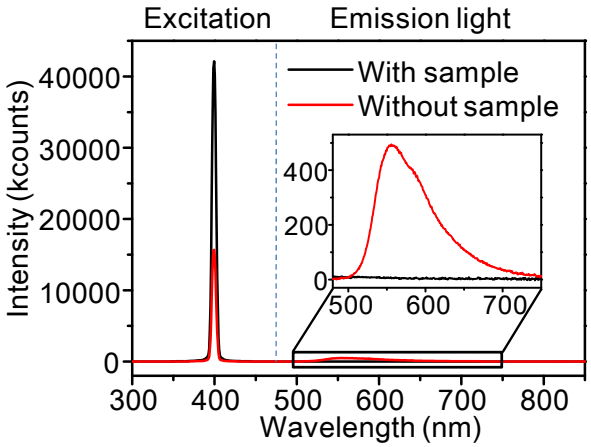

$$\phi = \frac{A_{em}}{A_{ex,\ without\ sample} - A_{ex,\ with\ sample}}$$

Sample	Quantum Yields (ϕ)
F8BT	37.5%

Fig. S1. Fluorescence quantum yield of F8BT film. $A_{ex,\ with\ sample}$ and $A_{ex,\ without\ sample}$ are the integrated intensity of the excitation light source peaked at 400 nm with and without sample, respectively, and A_{em} is the integrated intensity of emission light of the sample. Inset: the enlarged emission spectrum.

Quantum yield measurements were performed using the absolute method on a C11347 from Hamamatsu equipped with an integrating sphere, a L11562 Xenon lamp and a CCD detector. The quantum yields were calculated by comparing the integral of emission and the absorption of excitation light. The F8BT emitted yellow fluorescence with a quantum yield of ~37.5% under the excitation of 400 nm light, which is favorable to afford the optical gain for lasing.

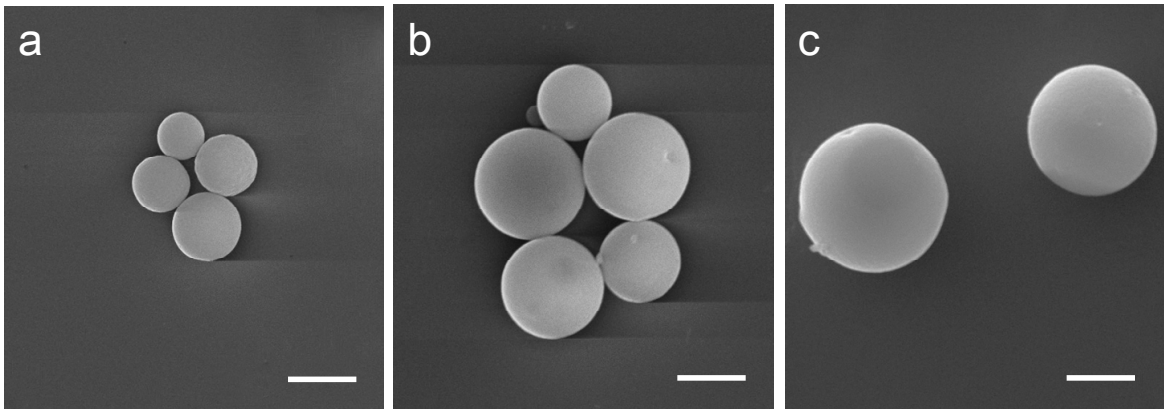

Fig. S2. SEM images of the polymer microspheres prepared by adding 200 µL F8BT chloroform solutions with consentrations of (a) 12.5, (b) 17.5, and (c) 22.5 mg/mL, respectively. All scale bars are 5 µm.

The diameter of the microspheres can be controlled from 4 to 11 µm by increasing concentration of F8BT in chloroform from 12.5 to 22.5 mg/mL. The images indicate that the products are spherical structures with a perfect circular boundary and smooth surface, which is beneficial for WGM resonance with high Q factors.

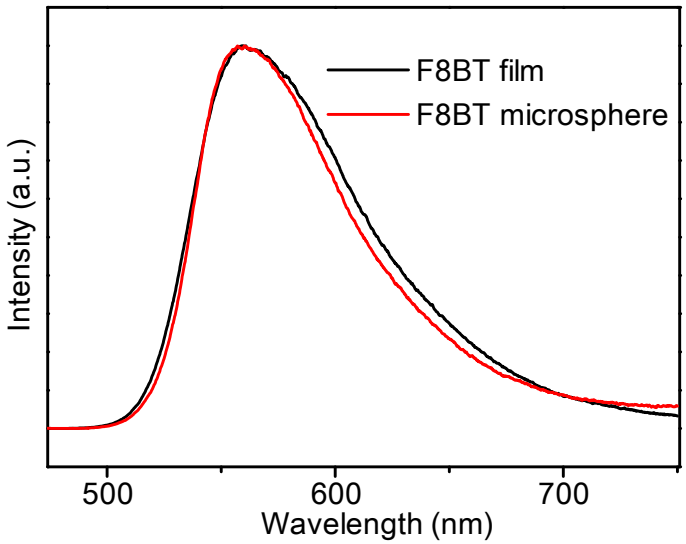

Fig. S3. Photoluminescence spectra of F8BT microspheres and F8BT thin film.

The fluorescence spectrum of the F8BT microsphere presents a single peak at 560 nm, which is consistent well with the spectra collected from the F8BT film.

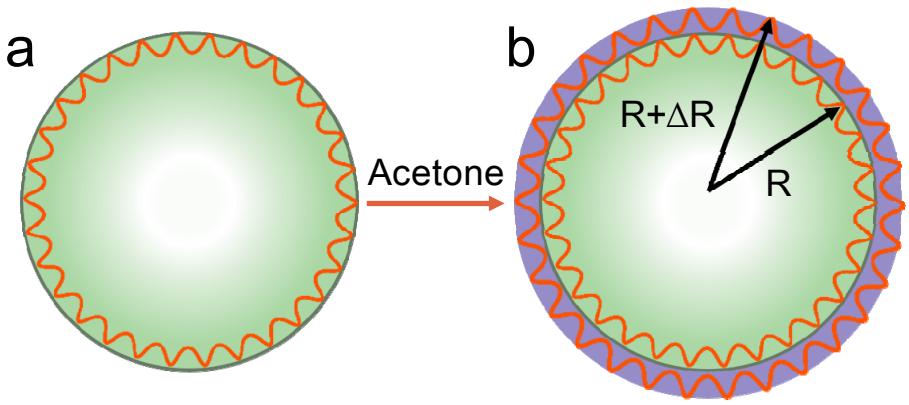

Fig. S4. Principle illustration of the chemical vapor sensors based on the organic WGM microlaser. (a) Bare sphere supporting a Whispering-gallery-mode. (b) WGM at the presence of an additional layer, ΔR, induced by chemiccal vapor adsorption.

When the surrounding environment was changed from air to acetone, the optical pass of microlaser increased due to the molecules attached on the surface, which results in a distinct red shift of the lasing modes, and can be utilized to monitor the acetone vapor.

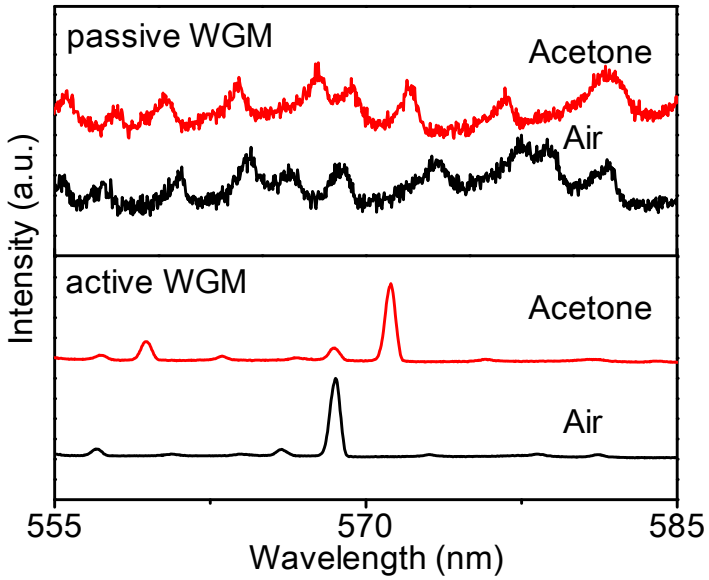

Fig. S5. The luminescence responses of the passive and active microcavities on acetone vapor.

Compared with the passive resonators, the active resonators have much narrower resonance linewidth, which brings much higher resolution in measuring the very small wavelength shift under very small amount of chemical vapors.

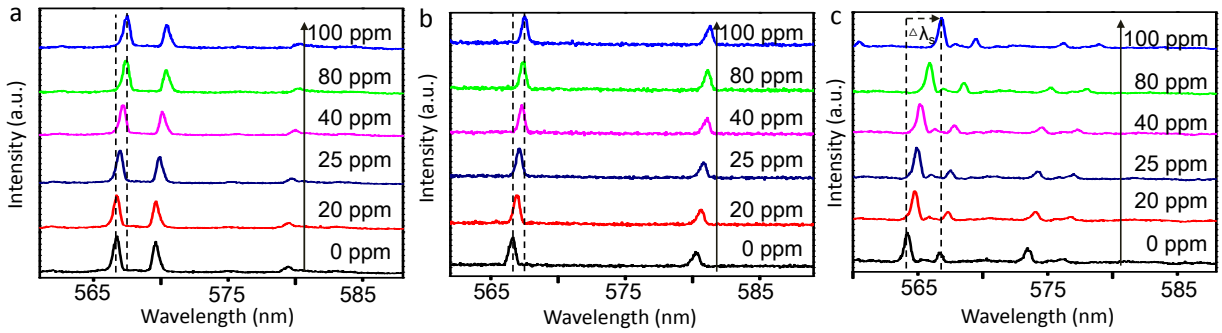

Fig. S6. Wavelength shift of the lasing mode under the exposure of different chemical gases. (a) methanol (b) ethanol, and (c) mixed solvent of ethanol and acetone solvent.

To better clarify the sensor mechanism of F8BT microspheres, we have further measured the responsiveness of the microlaser to other chemical vapors. As shown in Fig. S6, when acetone was replaced with methanol, ethanol or mixed solvent of ethanol and acetone, the lasing modes also gradually red shift with increasing the solvent concentration. Currently, we cannot differentiate the kind of the chemical gases. The high material compatibility of organic materials made it possible to functionalize the resonators with optical medium that is selectively responsive to a specific solvent. We believe a large number of high-selective and novel optical sensors would appear in the near future.

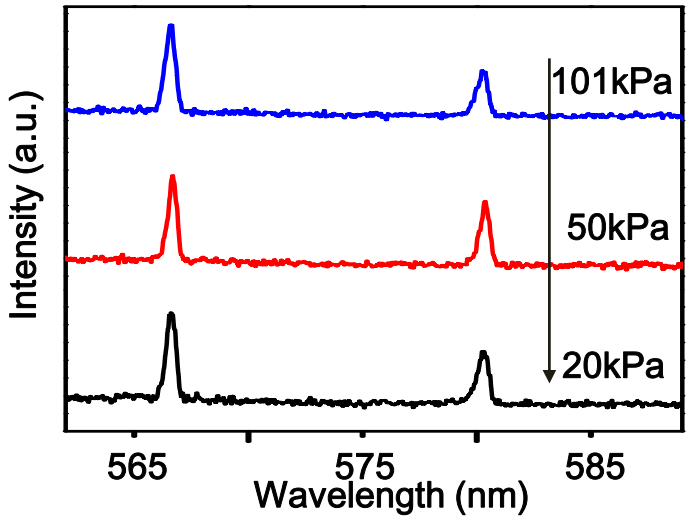

Fig. S7. Wavelength shift of the lasing mode under different pressures in air.

The lasing mode didnot show any detectable change with decreasing the pressure in air, indicating that the pressure has negligible effect on wavelength shift.

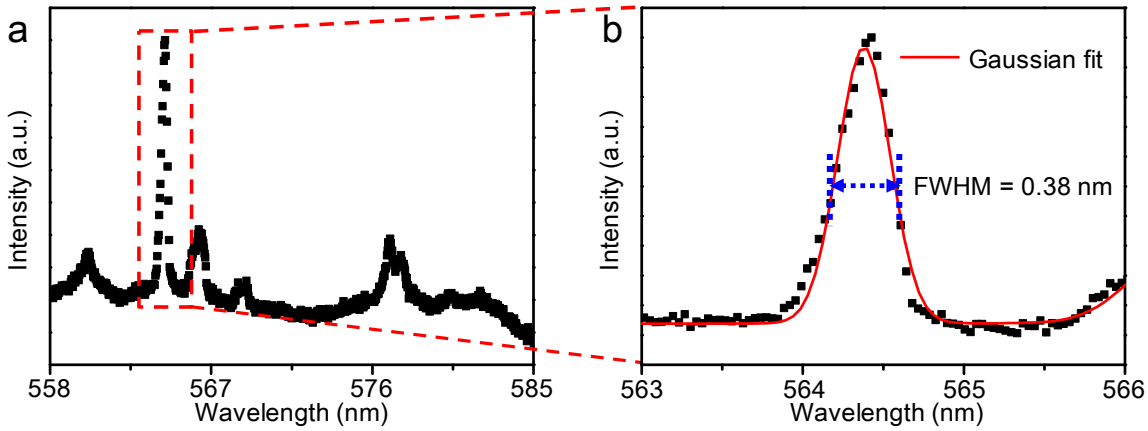

Fig. S8. Lasing spectra from the microlaser sensor in air (a) and a magnified view of the highest intensity lasing peak (b).

The spectrum linewidth of the microlaser sensor was 0.38 nm obtained from a Gaussian fit. Given that the noise level allows to determine a wavelength shift with a precision of 1/20 of the linewidth, the limit of detection with the WGM lasing response is calculated to be 90 ppb.

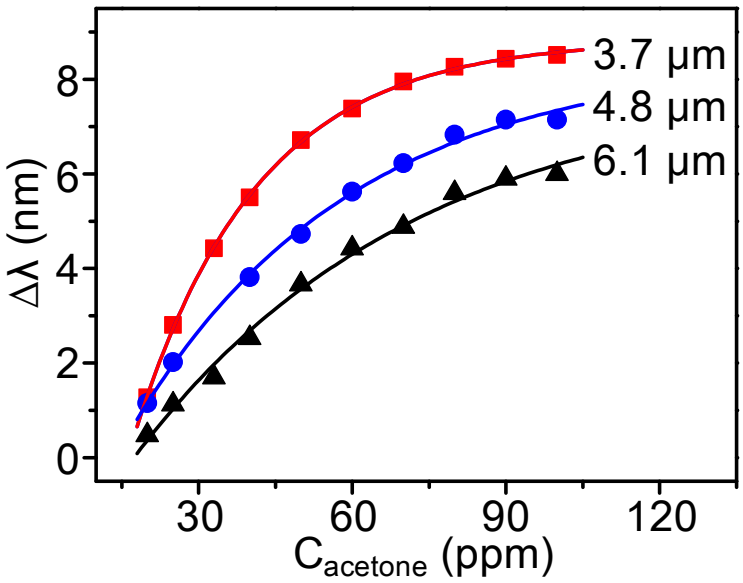

Fig. S9. Acetone dose response of the microspheres sensors with different diameters.

We collected the response wavelength-shift signals of microspheres with three different diameters under various gas concentrations. The results indicate that the smaller microsphere exhibited larger lasing wavelength shift, which provides a useful enlightenment for the improvement of sensitivity.

Fig. S10. Photograph of the F8BT microemulsion.

The formation of a uniform and stable yellow microemulsion under continuous stir demonstrates that F8BT were completely introduced into the hydrophobic interior of the CTAB micelles to form microspheres.

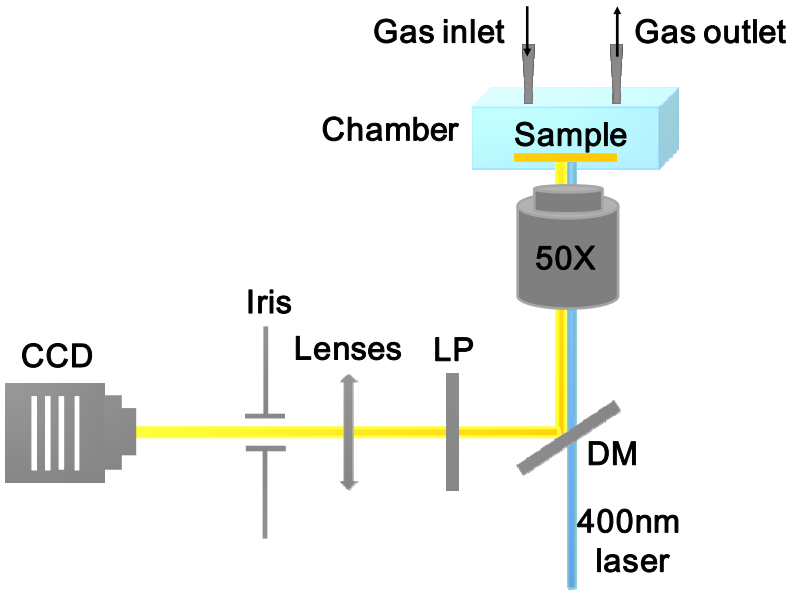

Fig. S11. Schematic demonstration of the experimental setup for the optical sensing measurements.

To exam the optical properties of the polymer microspheres, the samples were excited locally with a 400 nm pulse laser beam (200 fs, 1000 Hz). The microsphere resonators were dispersed on a glass substrate (refractive index about 1.5). The PL signal was collected by an objective lens (50×, numerical aperture 0.8), passed through the dichroic mirror (DM 400 nm), then a 420 nm longpass emission filter to eliminate the exciter light, focused by a group of lenses onto a confocal iris. The output signal can be spatially selected by the iris and recorded using a spectrometer.